Modeling,Simulation and Optimal Control for an Aircraft of Aileron-less Folding Wing

ZHENG JIE WANG[1], SHIJUN GUO[2] ,WEI LI [3]
1. School of Aerospace and Science Engineering
Beijing Institute of Technology
Beijing, 100081
CHINA
wangzhengjie@bit.edu.cn
2. Department of Aerospace Engineering
Cranfield University
Cranfield, Bedford, MK43 0AL, UK
s.guo@cranfield.ac.uk
3. Research Institute of Electric Science and Technology
University of Electric Science and Technology of China
Chengdu, Sichuan, 610054
CHINA
aegeanwei@gmail.com

Abstract: The purpose of this paper is to discuss the method of modeling and control system design for a loitering aircraft of aileron-less folding wing. A nonlinear model of the aircraft was established, and then linearized by small disturbance method. The lateral-directional stability augmentation options were analyzed through the root locus plots. The pole placement method based on linear quadratic regulator (LQR) technology was used to achieve desirable dynamic characteristics. In the analysis, the state parameters which represent rapid oscillation states of the aircraft such as roll rate and yaw rate were set as primary control parameters in the inner loop. The states oscillated slowly such as rolling angle and yaw angle were set as main control parameters in the outer loop. Based on the self-organizing fuzzy control algorithm, the aircraft can be controlled to fly in a desired path. Two types of course control plan were investigated and verified. The results show that the control plans are feasible and the control system is adequately robust to meet the requirements of the course control

Key-words: loitering aircraft, pole placement, LQR, fuzzy control, bank-to-turn (BTT), skid-to-turn (STT)

Nomenclature

A	State matrix
b	Wing span
C	Output matrix
D	Direct matrix
C_y	Lateral force coefficient
C_l	Rolling moment coefficient
I_x	Moment of inertia in roll
I_{xz}	Product of inertia about *ox* and *oz* axes
K	Feedback gain matrix
L	Lift: Rolling moment
m	Mass
N	Yawing moment
p	Roll rate
r	Yaw rate
R	Radius of turn
S	Wing reference area

u	Input vector
v	Lateral velocity
V	Total velocity
x	State vector
Y	Lateral force
y	Output vector
ζ	Rudder angle
η	Elevator angle
β	Sideslip angle
Φ	Roll angle

1 Introduction

A light weight small loitering aircraft of aileron-less folding back wing as shown in Fig.1 has been considered in this paper. It is designed to be carried by a large aircraft and cast over the target area. It could loiter autonomously in slow speed as a small UAV when the wing and the tail are unfolded [1] as illustrated in Fig.2. The aircraft loiters in the anticipated course which is indicated by lines between the contiguous navigation waypoints in the loitering stage as illustrated in Fig.3. The crucial task of the control system is to generate the control command based on the aircraft position and navigation deflection signal from the navigation system. The ideal control command will make the actual flight course identical to the desirable in order to accomplish the scheduled flight mission.

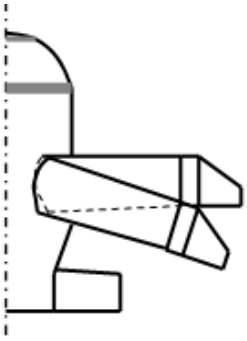

Fig.1 A loitering aircraft

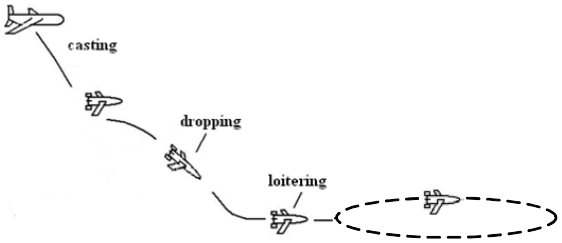

Fig.2 Loitering performing process

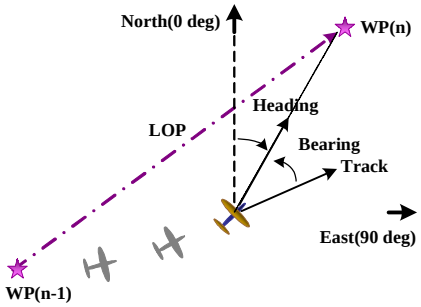

Fig.3 Navigation waypoints

The challenge of the control system design is how to satisfy the requirements of lateral maneuverability in order to accomplish the scheduled flight mission. Due to the light weight, small size and low velocity of the aircraft, it is prone to disturbance airflow. The lift coefficient varies with the angle of attack affected by the wing deformation. These factors make it difficult to achieve a satisfied controller design by classical control theory. It is therefore necessary to utilize flight control algorithm such as fuzzy logic, neural network, genetic algorithm, pattern recognition or other knowledge-base system to design the control system.

This current investigation firstly focused on establishing the lateral nonlinear model and the lateral control strategy. Attention was then paid to the design of the control system by utilizing the LQR state feedback method and self-tuning fuzzy control algorithm. Finally, mathematic simulation was carried out in Matlab/Simulink environment.

2 The Equations of Motion

The Newton's second law of motion for each of the six degrees of freedom simply states:

mass*acceleration=disturbing force

For the rotary degrees of freedom the mass and acceleration become moment of inertia and angular acceleration respectively whilst the disturbing force becomes the disturbing moment or torque. Thus the derivation of the equations of motion can be expressed in terms of the motion variable. The equations of motion in longitudinal and lateral dynamics are fully coupled.

For the vast majority of aircrafts when small perturbation transient motion is considered, longitudinal-lateral coupling is usually negligible. Consequently it is convenient to simplify the equation by assuming that longitudinal and lateral motions are in fact fully decoupled.

2.1 The lateral-directional equations of motion

In the most general form, the dimensional decoupled equations of lateral-directional motion is further simplify as

$$\begin{aligned} &m\dot{v}-\overset{\circ}{Y}_{\beta}\beta-\overset{\circ}{Y}_{p}p-(\overset{\circ}{Y}_{r}-mU_{e})r-mg\phi=\overset{\circ}{Y}_{\eta}\eta+\overset{\circ}{Y}_{\zeta}\zeta \\ &-\overset{\circ}{L}_{\beta}\beta+I_{x}\dot{p}-\overset{\circ}{L}_{p}p-I_{xz}\dot{r}-\overset{\circ}{L}_{r}r=\overset{\circ}{L}_{\eta}\eta+\overset{\circ}{L}_{\zeta}\zeta \\ &-\overset{\circ}{N}_{\beta}\beta+I_{xz}\dot{p}-\overset{\circ}{N}_{p}p-I_{z}\dot{r}-\overset{\circ}{N}_{r}r=\overset{\circ}{N}_{\eta}\eta+\overset{\circ}{N}_{\zeta}\zeta \end{aligned} \quad (1)$$

Where

$$\overset{\circ}{Y}_{p}=C_{y_p}\frac{1}{2}\rho V^2Sb,\ \overset{\circ}{L}_{p}=C_{l_p}\frac{1}{2}\rho V^2Sb^2,\ \overset{\circ}{Y}_{\zeta}=C_{y_\delta}\frac{1}{2}\rho V^2S$$

are lateral aerodynamic derivatives. For a small perturbation, the rolling rate is related to the attitude rate by $\dot{\phi}=p$.

The motion of the system is expressed in a *state space* form:

$$\dot{\mathrm{x}}=\mathrm{Ax}+\mathrm{Bu}$$

$$\begin{bmatrix}\dot{\beta}\\ \dot{p}\\ \dot{r}\\ \dot{\phi}\end{bmatrix}=\begin{bmatrix}y_\beta & y_p & y_r & y_\phi\\ l_\beta & l_p & l_r & 0\\ n_\beta & n_p & n_r & 0\\ 0 & 1 & 0 & 0\end{bmatrix}\begin{bmatrix}\beta\\ p\\ r\\ \phi\end{bmatrix}+\begin{bmatrix}y_\eta & y_\zeta\\ l_\eta & l_\zeta\\ n_\eta & n_\zeta\\ 0 & 0\end{bmatrix}\begin{bmatrix}\eta\\ \zeta\end{bmatrix} \quad (2)$$

Where the coefficients of state matrix A is the aerodynamic stability derivatives in concise form and the coefficients of the input matrix B are the control derivatives also in concise form. For example, $y_\beta=\overset{\circ}{Y}_{\beta}\big/m$, $l_p=(I_z\overset{\circ}{L}_{p}+I_{xz}\overset{\circ}{N}_{p})\big/(I_xI_z-I_{xz}^2)$, $y_\zeta=\overset{\circ}{Y}_{\zeta}\big/m$ with more details in reference[2].

Lateral derivative data are obtained from wind tunnel and used to illustrate the state equation. The flight speed is Mach 0.3 and the altitude is 250m. Table 1 presents some technical data of the aircraft. The dimensionless lateral derivatives are given in table 2. Any missing aerodynamic derivative is assumed to be negligible, hence set zero.

Table 1. Technical data of the aircraft

m (kg)	S (m^2)	I_x (kgm^2)	I_z (kgm^2)	I_{xz} (kgm^2)	b (m)	V (m/s)
60	2.2	84	50	9	4.2	89

Table 2. The dimensionless lateral derivatives

$C_{y\beta}$	C_{yp}	C_{yr}	$C_{y\eta}$	$C_{y\zeta}$
-0.02	-0.188	0.876	-0.007	0.0822

$C_{l\beta}$	C_{lp}	C_{lr}	$C_{l\eta}$	$C_{l\zeta}$
-0.005	-0.443	0.063	0.051	0.015

$C_{n\beta}$	C_{np}	C_{nr}	$C_{n\eta}$	$C_{n\zeta}$
0.005	-0.052	-0.378	0.01	-0.045

Substituting the above values into the lateral state equation (2), the linear decoupled state equation is:

$$\begin{aligned}\dot{\mathrm{x}}&=\mathrm{Ax}+\mathrm{Bu}\\ \mathrm{y}&=\mathrm{Cx}+\mathrm{Du}\end{aligned} \quad (3)$$

Where $\mathrm{x}=\left[\beta\ ,\ p\ ,\ r,\phi\right]^T$, $\mathrm{u}=\left[\delta_\eta\ ,\ \delta_\zeta\right]^T$.

$$\mathrm{A}=\begin{bmatrix}-0.1177 & -0.0077 & -0.9639 & 0.0327\\ 27.2317 & -16.5995 & 2.1438 & 0\\ 6.8119 & -1.4284 & -1.8904 & 0\\ 0 & 1 & 0 & 0\end{bmatrix}$$

$$\mathrm{B}=\begin{bmatrix}0.0449 & 0.4836\\ -40.3786 & 76.6806\\ -5.3566 & -27.9850\\ 0 & 0\end{bmatrix}$$

$\mathrm{C}=eye_{4\times4}$, $\mathrm{D}=zeros_{4\times2}$

The transfer functions of rolling state parameters corresponding to the control signals could be obtained from the above state equation:

$$\frac{\Delta\beta}{\Delta\delta_\eta}=\frac{0.04493s^3+6.301s^2+31.02s-2.87}{s^4+18.61s^3+43.39s^2+75.18s-2.16}$$

$$\frac{\Delta\phi}{\Delta\delta_\eta}=\frac{-40.38s^2-91.35s-131.9}{s^4+18.61s^3+43.39s^2+75.18s-2.16}$$

$$\frac{\Delta p}{\Delta\delta_\eta}=\frac{-40.38s^3-91.35s^2-131.9s-1.942e-006}{s^4+18.61s^3+43.39s^2+75.18s-2.16}$$

$$\frac{\Delta r}{\Delta\delta_\eta}=\frac{-5.351s^3-31.57s^2+0.6566s-4.222}{s^4+18.61s^3+43.39s^2+75.18s-2.16}$$

$$\frac{\Delta\beta}{\Delta\delta_r}=\frac{0.4836s^3+35.34s^2+571.9s+2.778}{s^4+18.61s^3+43.39s^2+75.18s-2.16}$$

$$\frac{\Delta\phi}{\Delta\delta_r}=\frac{76.69s^2+107.2s+1280}{s^4+18.61s^3+43.39s^2+75.18s-2.16}$$

$$\frac{\Delta p}{\Delta\delta_r}=\frac{76.69s^3+107.2s^2+1280s+1.931e-005}{s^4+18.61s^3+43.39s^2+75.18s-2.16}$$

$$\frac{\Delta r}{\Delta\delta_r}=\frac{-28s^3-574.1s^2-41.62s+41.98}{s^4+18.61s^3+43.39s^2+75.18s-2.16}$$

In factorized form the lateral-directional characteristic equation is

$$\Delta(s)=(s+16.22)(s-0.02826)(s^2+2\times2.17\times0.557s+2.17^2)=0$$

Therefore, there are three modes of lateral movement [2]: one is a rolling converge mode which attenuates rapidly corresponding to a big negative root s=-16.22. The roll mode time constant (T_r) is 0.062 s; The second is a spiral mode which diverges slowly with rolls and yaws but without sideslips corresponding to a characteristic root closed to the origin s=0.0283. The spiral mode time constant(T_s) is 35.36 s. Clearly, the spiral mode here is unstable; The third is the dutch roll mode which is oscillating in high frequency with medium damping corresponding to a pair of characteristic conjugate roots $s_{1,2}$ = -1.2088 ± j1.8029.The dutch roll damping ratio(ξ_d) is 0.557 and the dutch roll undamped natural frequency ω_d is 2.17rad/s.

2.2 Model analysis and Lateral-direction stability augmentation

The lateral-directional stability augmentation options are summarized in Fig.4 in which it is implied that a negative feedback loop may be closed between any of the motion variables and either the difference or rudder.

In the following catalogue of root locus plots each plot illustrates the effort of a single feedback loop closure as a function of increasing feedback gain *K*.

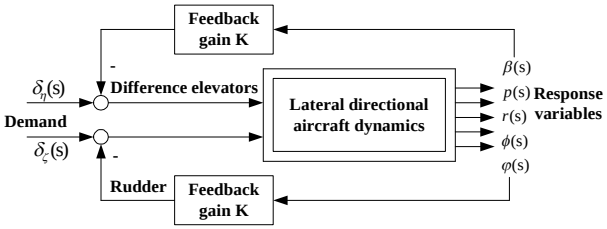

Fig.4 Lateral-directional feedback options

(1) Roll attitude feedback to differential elevators

The open loop transfer function is

$$\frac{\phi(s)}{\delta_\eta(s)}=\frac{(s+1.1311-j1.4096)(s+1.1311+j1.4096)}{(s+16.2213)(s-0.0283)(s^2+2\times0.557\times2.17s+2.17^2)}$$

The corresponding root locus is shown in Fig.5. The dutch roll mode pole is approximately cancelled by the numerator zero. This means that this mode is insensitive to this feedback option. The roll mode stability increases rapidly as the gain *K* is increased since its pole moves to the left on the s-plane. The roll mode is most sensitive to this feedback option. However, the spiral mode remains unstable at all values of *K*.

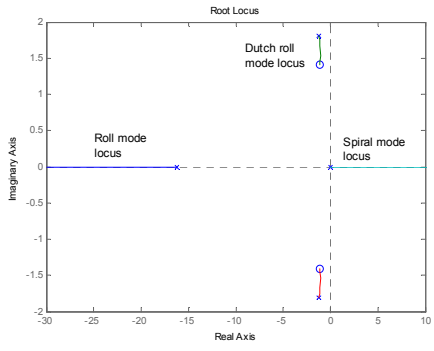

Fig.5 Roll attitude feedback (*-open loop poles, o -open loop zeros)

(2) Roll attitude feedback to rudder

The open loop transfer function is

$$\frac{\phi(s)}{\delta_\varsigma(s)}=\frac{(s+0.6989-j4.0252)(s+0.6989+j4.0252)}{(s+16.2213)(s-0.0283)(s^2+2\times0.557\times2.17s+2.17^2)}$$

The corresponding roll attitude feedback to rudder root locus plot is shown in Fig.6. The dutch roll poles are approximately cancelled by the numerator zeros which implies that the mode is insensitive to this feedback option. As *K* is increased the spiral mode pole moves to the left on

the s-plane and its stability increases very rapidly. At the value of K=0.642, the spiral and roll modes couple to form a low frequency oscillatory characteristic. Therefore, roll mode stability decreases rapidly as the gain K is increased until its poles couples with that of the spiral mode. The negative roll attitude feedback to rudder is a kind of lateral pendulum mode.

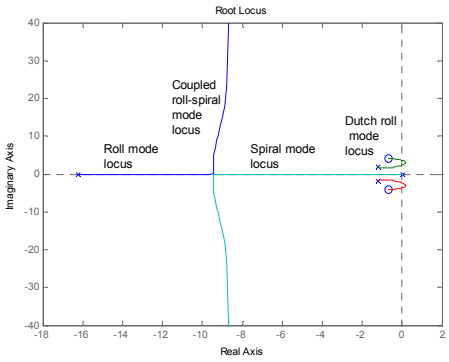

Fig.6 Roll attitude feedback

(3) Roll rate feedback to rudder

The open loop transfer function is

$$\frac{p(s)}{\delta_{\zeta}(s)} = \frac{s(s+0.6989-j4.0252)(s+0.6989+j4.0252)}{(s+16.2213)(s-0.0283)(s^2+2\times0.557\times2.17s+2.17^2)}$$

The corresponding roll attitude feedback to rudder root locus plot is shown in Fig.7.The roll mode stability increase rapidly as the gain K is increased since its pole moves to the left on the s-plane. The dutch roll mode is sensitive to this feedback option too. However, the spiral mode remains unstable at all values of K. So negative roll rate feedback to rudder is equivalent to an increase in the yaw damping properties of the wing.

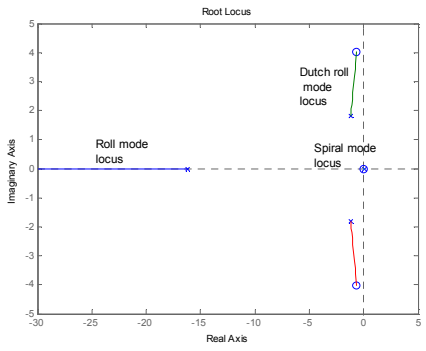

Fig.7 Roll rate

3 Control Strategy Design

To make sure the aircraft fly through the scheduled navigation waypoints on the great circle flight path as showed in Fig.3, an onboard navigation system detects the track angle deflection $\Delta\chi$ = *Track-Heading*. The task of flight track control is to minimize the deflection, and make the aircraft fly through the scheduled navigation waypoints along the shortest path.

3.1 Bank-to-turn control strategy

Bank-to-turn control means that the lift vector is always towards the direction of target by banking the fuselage during flight as shown in Fig.8. The pitch angle and roll angle change together to make the necessary maneuver and acceleration quickly in the desirable direction. In the same time, the sideslip angle should be reduced down to zero[3].

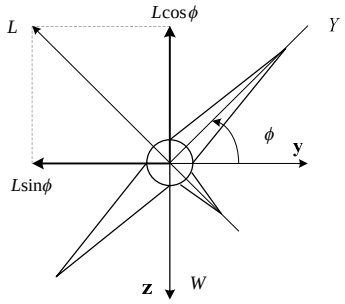

Fig.8 Force components during bank-to-turn

In Fig.8, the force equilibrium equations in the direction Oz_b and Oy_b are expressed by:

$$\sum F_Z = 0 \Rightarrow L\cos\phi + Y\sin\phi = W \tag{4}$$

$$\sum F_y = 0 \Rightarrow Y\cos\phi + \frac{mV^2}{R} = L\sin\phi \tag{5}$$

When no sideslip angle is generated in the band-to-turn process, the lateral maneuverable force is provided by the horizontal component of the lifting force rather than the side force. The above equation becomes:

$$L\sin\phi = \frac{mv^2}{R} = mv\dot{\psi}_s \tag{6}$$

The relationship between the turning angle rate $\dot{\psi}_s$ and roll angle is written as:

$$\dot{\psi}_s = \frac{L\sin\phi}{L\cos\phi v}\mathrm{g} \approx \frac{\mathrm{g}\phi}{v} \tag{7}$$

During the aircraft turning, the flight course angle rate $\dot{\chi}$ equals to $\dot{\psi}_s$, hence:

$$\dot{\chi} \approx \frac{\mathrm{g}\phi}{v} \tag{8}$$

Through Laplace transformation, the flight course angle is expressed by:

$$\chi(\mathrm{s}) = \frac{g\phi}{vs} \tag{9}$$

When the flying direction needs to be altered or the aircraft is hovering to turn, the autopilot manipulates the rolling channel to make the maneuvering. Then the primary lifting surface is manipulated towards the target in order to produce the acceleration in normal direction as great as possible; the autopilot manipulates the yawing channel to ensure the lateral acceleration n_z and the sideslip angle β equal to zero. To achieve the aircraft rolling without ailerons, this paper presents a method of control by operating the elevators independently. The control strategy is shown in Fig.9.

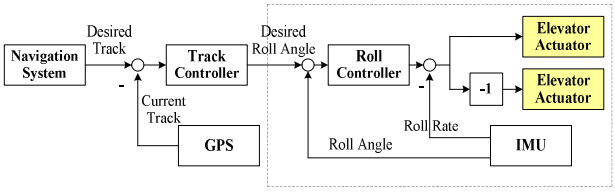

Fig.9. Bank-to-turn control strategy

Due to the structure attributes of the aircraft and its manipulation process in the bank-to-turn, some characteristics are noted: a significant coupling in the channels of pitch, yaw and roll; a sideslip angle close to zero and a strong maneuver capability

3.2 Skid-to-turn control strategy

For an axis symmetric aircraft in aerodynamic configuration, STT control method is generally adapted to alter sideslip angle and adjust the horizontal navigation track by manipulating the rudder. The aircraft using STT has a stable roll channel and minimum coupling between pitch, yaw and roll channels. For a plane-symmetric aircraft considered in this paper, it is proposed to adapt a skid-to-turn strategy as shown in Fig.10 to prove the control capability. The difference elevator control make the rolling angle equal to zero; the rudder controls the horizontal maneuver of the aircraft.

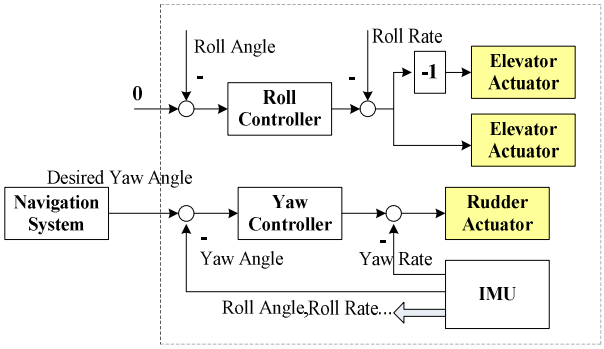

Fig.10 Skid-to-turn control strategy

When the aircraft flies at a large angle of attack in the STT mode, a great sideslip angle generates severely asymmetric eddy. This would produce a big harmful roll and yaw moments, which might exceed the allowed limit of the control system. In addition, the pitch and the yaw autopilots utilize their independent control systems and the direction of maneuver lies in the composed direction of attack angle vectors. When the angle of attack is getting greater gradually, an increasing dynamic coupling and an inertial coupling would be generated in pitch channel and yaw channel. Accordingly, the maneuver ability is undermined.

4 Control System Design

No matter which plan is adapted, the control system design mainly includes a few control loops: the rate damping loop, attitude stabilizing loop and flight path track loop[4].

4.1 Rate damping design based on the pole placement method

An alternative and very powerful method for

designing the above feedback gains systems is the pole placement method [5].

The state and output matrix equations are described in equation(3).Assuming that augmentation is achieved by negative feedback of the state vector x(t) to the input vector u(t) then the control law may be written

$$u(t)=v(t)-Kx(t) \qquad (10)$$

where,v(t) is a vector of input demand variables and *K* is a matrix of feedback gains. The closed loop state and output equations are:

$$\begin{aligned}\dot{x}(t)&=(A-BK)x(t)+Bv(t)\\ y(t)&=(C-Dk)x(t)+Dv(t)\end{aligned} \qquad (11)$$

Now the characteristic equation of the augmented aircraft is given by

$$\Delta(s)=\left|sI-(A-BK)\right|=0$$

Thus if the required stability and control characteristics of the augmented system are specified, the equation may be solved to find K. This means that the poles of the closed loop system may be placed on the s-plane exactly as required.

The LQR methodology is adapted in the design of state feedback gains to improve the dynamic characteristics and meet the predefined performance index of the aircraft.

LQR optimal design may be described as if the system departs from the equilibrium state x=0 for some reason, the control will make the state x(t) return to its equilibrium state x=0 in a optimal route or manner. In addition, the demand for control power will be constrained. The objective function can be expressed in a general form as:

$$J(u)=\frac{1}{2}\int_{t_0}^{t_1}[x^T(t)Q(t)x(t)+u^T(t)R(t)u(t)]dt \qquad (12)$$

Where *Q(t)* and *R(t)* are weight matrix for different objectives of "returning to the equilibrium point" and "minimum control power demand"[6].

The state feedback control law is u= *-K * x*, where *K* is the gain matrix for the state feedback which can be designed by using LQR function in MATLAB. The weight matrix *Q(t)* **=** diag[0,q1,0,q2] is a diagonal with q1=500 , q2=300. Then the optimal state feedback gain matrix could be:

$$K=\begin{bmatrix}-0.0866 & -10.3439 & -0.0408 & -8.0543\\ 0.3088 & 19.6188 & 0.0055 & 15.3339\end{bmatrix}$$

Fig.11 shows the step response of four states corresponding to two control variables when there is no control input. The step response closed loop system with a state feedback is shown in Fig.12.

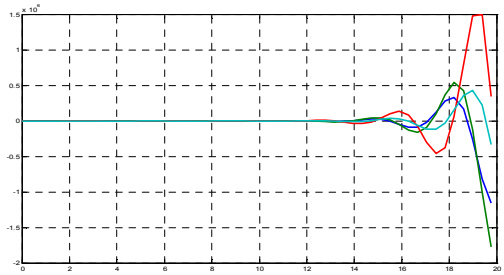

Fig.11 Step response(no control input)

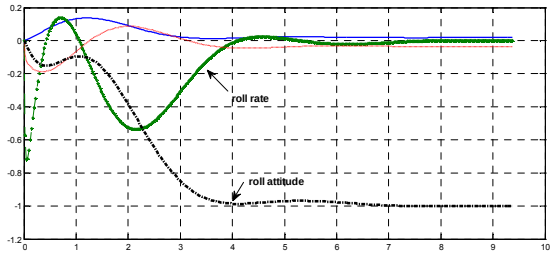

Fig.12 Step response through state feedback

Obviously, after the configurations of poles are accomplished through state feedback, the damping traits had been improved, and responses of attitudes had become stable to make the aircraft quickly respond to the guidance command provided by the fight path track loop.

4.2 Self-tuning fuzzy control design

Fuzzy control is suitable for a complicated control object requiring fast and effective control process[7,8]. For the current complicated system of multiple variables, high-order, nonlinearity however, it is difficult to summarize the practicable fuzzy control law. In this case, a self-organizing fuzzy controller which is capable of auto-adjusting and enhancing the fuzzy control laws is desirable. To design such a self-organizing fuzzy controller, the

main tasks are to adjust the scaling factor and tuning factor to meliorate the control performance [9].

(1) Scaling factor

Let k_e and k_c denote the scaling factor of the deflection and its change rate respectively. Its value could be determined following a guideline in general cases: when the deflection is large, a small k_e should be chosen to make the system respond quickly but not result in too much overshoot; as the deflection reduces, k_e should be gradually increased to improve the steady-state accuracy. The effect of k_e adjusting is equivalent to altering the universe of deflection in order to achieve the dynamic characteristic improvement and steady-state accuracy enhancement.

Let Δk_e denote the increment of k_e, it forms a relationship with the gain of deflection Δx. When k_e is increased up to k_{max} when the deflection is stabilized in a steady-state deflection range, the relationship between Δk_e and Δx is purely linear. In this case, Δk_e can be expressed as:

$$\Delta K_e = k\Delta x\left(2-\frac{K_e}{K_{max}}\right) \tag{13}$$

When $\Delta x \to 0$, we could get the derivative format:

$$dK_e = kdx\left(2-\frac{K_e}{K_{max}}\right) \tag{14}$$

After integrating, we obtain:

$$K_e = K_{max}\left(2-e^{\frac{k|x|+c}{-K_{max}}}\right) \tag{15}$$

Where c is an integral constant. When the deflection becomes negligible, k_e is equal to k_{max} and $kx+c=0$. In this case, we may assume $c=0$ and thus

$$K_e = K_{max}\left(2-e^{\frac{-k}{K_{max}}|x|}\right) \tag{16}$$

When k_e is affirmed, $k_c=\beta k_e$, k_{max}, k and β are optimized by a simplex method, where the objective function is $J=\int_{t_0}^{t_f} t\left|x(t)\right|dt$. Then k_{max}, k and β could get their optimal value. Accordingly, as a consecutive function of the deflection, the self-adjusting functions of k_e and k_c can be determined.

(2)Tuning factor

In the fuzzy control model with tuning factor, the control signal could be set as:

$$U=-\left(\alpha\cdot x+(1-\alpha)\cdot\dot{x}\right),\alpha\in(0,1) \tag{17}$$

Where, α is tuning factor; x and $\dot{x}$ are the deflection and its change rate respectively. Tuning the α magnitude could alter the weighting of the deflection and its change rate. Similar to the deduced process of self-adjusting scaling factor, the self-adjusting tuning factor can be deduced by $\alpha=1-e^{-k|x|p}$. Similarly, by setting $J=\int_{t_0}^{t_f} t\left|x(t)\right|dt$ as the objective function, k and p could be optimized by a simplex method to determine the function of self-adjusting tuning factor.

From the basic theory of fuzzy controller, fuzzy control has the attributes of proportional control and derivative control without the integral process compared to the classical PID control [10]. Thereby, it is desirable to blend the integral into the fuzzy controller design to improve the steady-state accuracy of fuzzy control. Fig. 13 shows the control loop diagram based on state feedback and self-organizing fuzzy control methodology.

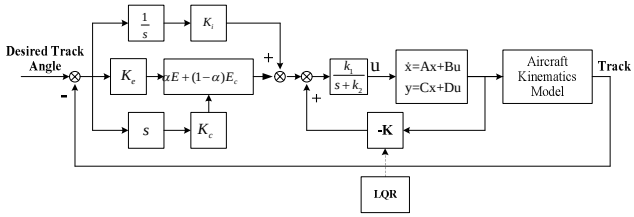

Fig.13 Diagram of control loop

5 Simulations

A small aircraft nonlinear simulation model of six degrees of freedom is built in the

MATLAB/Simulink. The forces and moments are the function of kinematic parameters such as airspeed, angle of attack, sideslip angle, roll angle and their derivatives. The nonlinear factors like nonlinear change of lift are accounted when building the model of aerodynamic forces and moments.

The process of level maneuver of a small aircraft is simulated at flight condition H_0=350m and V_0=80 m/s; the yaw, pitch and roll are initialized at 0^o. The time of simulation lasts 30s, t=30s. The control command is given as: heading angleχ=5°.

5.1 Simulation results of bank-to-turn

Taking the nonlinear model of six degrees of freedom as the control object, the bank-to-turn simulation software is written in C-language and built in Simulink as shown in Fig.14. MATLAB calls the C-program utilizing mex-Function tool. To account for the saturation of the actuator and dynamic response characteristics, all of the actuators are modeled as first-order lags with a gain and limits on deflection and rates. The result of control is shown as in Fig.15.

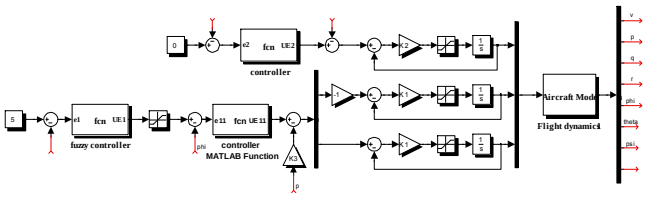

Fig.14 bank-to-turn simulation based on Simulink

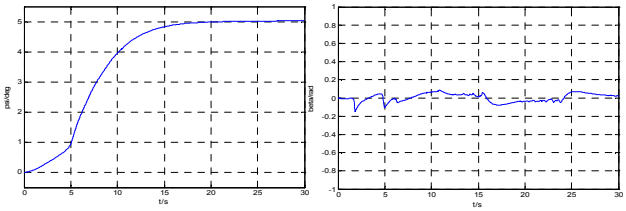

(a) Heading angle (b) Sideslip angle

Fig.15 BTT simulation results

5.2 Simulation result of skid-to-turn

For the autopilot of the BTT aircraft, the most important task is to restrict the sideslip angle in the allowed range. Otherwise, when the sideslip angle and the angle of attack are large enough, rolling moment would be generated to aggravate the coupling. For the autopilot of the STT aircraft, it is necessary to reduce the rolling angle and its rate down to zero to decouple the three control channels.

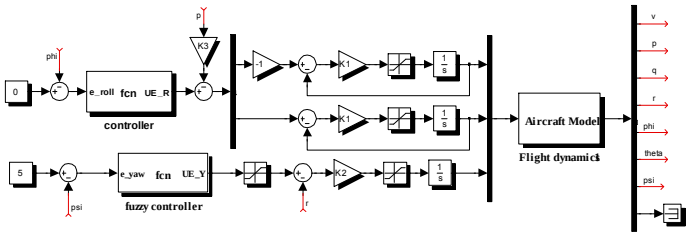

Fig.16 Skid-to-turn simulation

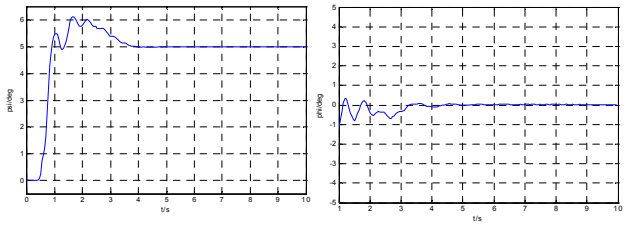

(a) heading angle (b) roll angle

Fig.17 STT simulation results

As shown in the above simulation results, the two turning modes have their own advantages and disadvantages: the bank-to-turn by a differential movement of the elevators appears in a more steady way. Due to a little rolling moment however, the heading angle responds slowly to the commands, as shown in Fig.15; the skid-to-turn by the deflection of rudder responds to the commands rapidly and could achieve steady state quickly. In the turning process however, the aircraft flies in an unstable state, and the heading angle has a large overshoot, as shown in Fig.16.

Theoretically, bank-to-turn could provide greater maneuver capability and faster response speed. For the aircraft without ailerons studied in this paper however, it is ineffective to accomplish bank-to-turn by using the differential movement of the elevators having a small control surface area. Meanwhile, it is easy to produce significant coupling among the three control channels and affect the control process and effectiveness. If the maneuverability demand is not too high, it is desirable to adapt the relatively simple STT control method.

6 Conclusions

In this paper, a linear and a nonlinear aircraft model without ailerons have been built for the aim of controller design and performance simulation. Firstly the flight track controller in a lateral decoupling mode has been designed for two kinds of turning modes. Based on the model and controller, the attitude of the entire control system was simulated.

The natures of the small aircraft such as nonlinearity and time-variation partly due to non-modularity in the aerodynamic characteristics and random effect in the flight environments make the control more complicated. The results show that the control system will be the essence of challenge for the small aircraft. Future work should focus on the research of advanced control algorithm to achieve optimal control.

References:

[1] Wu G.H., Wang Z.J. and Fan N.J., Control Method of Dynamic Inversion with Neural Network Used for MAV, *Journal of Astronautics*, Vol.s1, 2008.

[2]Cook,M.V., Flight Dynamics Principles, Butterworth-Heinemann,pp.174-206.

[3]Tong,C.X., Wang, Z.J. and Zhang,T.Q., Decoupling System Design Based on Variable Structure System for BTT Missile,*Journal of Astronautics*,Vol.1,2006.

[4]Kulczycki, E. A., Joshi ,S. S., and Hess ,R. A. , Towards Controller Design for Autonomous Airships Using SLC and LQR Methods. *AIAA Guidance,Navigation, and Control Conference and Exhibit*,AIAA-2006-6778, 21-24 Aug. 2006, Keystone,Colorado.

[5] Mariun, N., Zulkifli,S.A., Hizam,H., Wahab,N.A., Design and Simulation of Pole Placement Controller for D – STATCOM in Power Quality Problems Mitigation, *WSEAS Transactions on Systems*, Issue 8, Vol.4, August 2005,pp.1298-1306.

[6]Na,S.,Librescu, L., Kim,M.H.,etc.,Robust aeroelastic control of flapped wing systems using a sliding mode observer, *Aerospace Science and Technology*,vol.10, 2006, pp.120-126.

[7]Srivastava,S., Bansal,A., Chopra,D., Goel, G.., Modeling and Control of a Choquet Fuzzy Integral Based Controller on a Real Time System, *WSEAS Transactions on Systems*, Issue 7, Vol. 5, July 2006,pp.1571-1579.

[8] Anis Sakly, Kamel Ben Othman and Mohamed Benrejeb, Mamdani Type Fuzzy Controllers for the Stabilization of Linear Systems, *WSEAS Transactions on Systems*, Issue 4, Vol. 2, October, 2003,pp.820-827.

[9]He, p.,Wang, H.X., Fuzzy Controller Design and appllication, *Science Press*, 1997.

[10]Zhang, T.Q., Luo, X.S. and Zhan L., Self-organizing Fuzzy Decoupling Control for Nonlinear System, *Computer Simulation*,Vol.1,2004 (in China).